Temporal transcriptomic dynamics of the ATX-LPAR-PLPP axis during skeletal muscle regeneration at single cell resolution

Osvaldo Contreras[a,b]

[a]Developmental and Regenerative Biology Division, Victor Chang Cardiac Research Institute, Darlinghurst, NSW 2010, Australia
[b]School of Clinical Medicine, UNSW Medicine & Health, St Vincent's Healthcare Clinical Campus, Faculty of Medicine and Health, UNSW Sydney, Kensington 2052, Australia

Correspondence:
o.contreras@victorchang.edu.au, oicontre@uc.cl
Twitter: @Osvaldoics (O. Contreras)
ORCID: https://orcid.org/0000-0002-8722-9371

Abstract

Lysophosphatidic acid (LPA) is a growth factor-like bioactive phospholipid. As such, it has recently become an attractive target during tissue inflammation, repair, and regeneration, demonstrating biomedical relevance. LPA and LPA receptor-mediated signalling pathways regulate embryonic development, wound healing, carcinogenesis, and fibrosis, inducing cell migration, proliferation, and differentiation. Extracellular LPA is produced by the secreted hydrolase ectonucleotide pyrophosphatase/phosphodiesterase 2 (Enpp2, Autotaxin/Atx) and hydrolyzed by different membrane-bound phospholipid phosphatases (PLPPs). This study uses bulk and single-cell RNA sequencing to explore the gene expression dynamics of LPA receptors (Lpa_{1-6}), Enpp2, and Plpp in skeletal muscle cells in homeostatic conditions and regeneration. Here, I show that skeletal muscle differentially expresses Lpar-Enpp2/Atx-Plpp coding genes, being *Lpar1* the highest expressed member among LPARs. *Lpar1* was highly expressed by FAPs and tenocytes, whereas *Enpp2*/Atx was mainly by FAPs. Clustering stromal fibro-adipogenic progenitors (FAPs) identified different populations representing distinct cell states with robust Lpar and Enpp2/Atx transcriptome signatures in homeostasis or resting-like cell states, including Dpp4+ and Hsd11b1+ FAPs. Tissue injury induces strong and fast repression of LPA receptors and Enpp2/Atx, indicating activated and proliferative FAP cell states are partly defined by a strong downregulation of LPAR and Enpp2/Atx gene expression. Hence, our results highlight the presence of the Atx-Lpar-Plpp axis in different muscle cells and FAP lineage in homeostasis and injury, providing a robust entry point for profound research on the role of LPA signalling skeletal muscle and other organs and tissues.

Keywords: Lysophosphatidic acid; Myogenesis; Muscle Stem Cells; LPAR Signalling; Fibro-adipogenic Progenitors; Regeneration; Tenocytes

Summary

Our single-cell omics approach revealed the involvement and temporal transcriptomic dynamics of the ATX-LPAR-PLPP axis in response to skeletal muscle regeneration.

Abbreviations

Autotaxin, ATX
Connective Tissue Growth Factor, CTGF/CCN2
Ectonucleotide pyrophosphatase/phosphodiesterase 2, ENPP2
Fibro-adipogenic progenitors, FAPs
G protein-coupled receptors, GPCRs
LPA receptors, LPARs
Lysophosphatidic acid, LPA
Mesenchymal stromal cells, MSCs
Muscle stem cells, MuSCs
Phosphatidic acid, PA
Phospholipid phosphatases, PLPPs

Introduction

Striated skeletal muscle is an endocrine organ regulating whole-body metabolism, heat, posture, and movement. This highly plastic tissue changes and adapts its function throughout an organism's lifespan, making it an essential organ to maintain homeostasis. Mammalian adult skeletal muscle regeneration remains one of the most captivating and remarkable faculties in mammals (Baghdadi and Tajbakhsh, 2018). Although regenerative muscle capability relies on tissue-resident adult unipotent muscle stem cells (MuSCs, also known as satellite cells) (Lepper et al., 2011; Murphy et al., 2011; Sambasivan et al., 2011; Fry et al., 2015), recent discoveries have demonstrated that successful muscle regeneration requires a complex set of different cell types [reviewed in (Theret et al., 2021)]. Although significant progress has been made in understanding skeletal muscle regeneration, there is a need to identify novel, potentially druggable targets to boost muscle repair in myopathies, neuromuscular disorders, muscle trauma, and unhealthy aging. Fibro-adipogenic progenitors (FAPs) have recently emerged as essential stromal cells for maintaining skeletal muscle homeostasis, mass, neuromuscular integrity, and proper tissue regeneration [reviewed in (Giuliani et al., 2021; Theret et al., 2021)]. However, FAPs have also been proven to drive muscle degeneration, mediating exacerbated fibrous-adipose-bone ectopic deposition in severe trauma and myopathies [reviewed in (Contreras et al., 2021b; Molina et al., 2022)].

Lysophosphatidic acid (LPA, also known as lysophosphatidate) is a small circulating bioactive phospholipid [430-480 Da, equivalent to 4-5 amino acids in Da size] with a core which has a phosphate group, glycerol, and a fatty acid chain (Moolenaar, 1995; Okudaira et al., 2010). LPA can act as an extracellular signalling molecule via autocrine, paracrine, or endocrine processes (Moolenaar, 1995; Geraldo et al., 2021). Among its wide range of biological functions, LPA regulates platelet aggregation, smooth muscle cell contraction, cell differentiation, cell proliferation and survival, chemotaxis, carcinogenesis, and stem cell biology (van Corven et al., 1989, 1992; Fang et al., 2000; Binder et al., 2015; Lidgerwood et al., 2018; Magkrioti et al., 2018; Geraldo et al., 2021; Xu et al., 2021). LPA signalling is mediated by at least six different receptors, which recognise extracellular LPA species (LPA_{1-6}, encoded by six *Lpar* genes in mice) (Kihara et al., 2014; Geraldo et al., 2021). These receptors are members of the seven-transmembrane G protein-coupled receptors (GPCRs) superfamily, Class A rhodopsin-like and lipid-like receptors (Kihara et al., 2014). As such, LPARs signal through several intracellular effector pathways activated by heterotrimeric G proteins, including $G_{i/o}$, $G_{12/13}$, $G_{q/11}$, and G_s [reviewed in (Geraldo et al., 2021)].

Extracellular levels of LPA are mainly controlled by its abundance and by the lysophospholipase D activity of the secreted enzyme Autotaxin (also known as Atx or Enpp2) (Akira et al., 1986; Tokumura et al., 2002; Okudaira et al., 2010). Enpp2/Atx generates LPA from lysophospholipids hydrolysis (lysophosphatidylcholine, lysophosphatidylserine and

lysophosphatidylethanolamine), making it an essential enzyme to produce and maintain extracellular and serum LPA (Umezu-Goto et al., 2002; Benesch et al., 2015). Enpp2/Atx is required for proper mammalian development and Enpp2/Atx-null mice die around embryonic day 10 (Tanaka et al., 2006). Although ubiquitously expressed in adult tissues (Ninou et al., 2018), recent studies have shown adipose tissue derived Enpp2/Atx as a major source of circulating and extracellular levels of this enzyme (Dusaulcy et al., 2011; Nishimura et al., 2014), suggesting Enpp2/Atx could act as an essential long and short distance adipokine intermediary (Funcke and Scherer, 2019).

Extracellular LPA is primarily metabolized by the ecto-activities of at least three plasma membrane-bound magnesium-independent lipid phosphate phosphatases or phospholipid phosphatase: Plpp1, Plpp2, and Plpp3, encoded by their respective Plpp genes [reviewed in (Brindley et al., 2009; Tang et al., 2015)]. However, other magnesium-independent phospholipid phosphatases with broad substrate specificity can also metabolize LPA, including Plpp4, Plpp5, and Plpp6 (Tang and Brindley, 2020). Plpp7 has no demonstrable enzymatic activity, and little information is available (Tang and Brindley, 2020). Plpps catalyze the dephosphorylation of various glycerolipid and sphingolipid phosphate esters, regulating their availability (Brindley et al., 2009). Because of their crucial role in metabolizing LPA, gaining knowledge about the gene expression dynamics of Enpp2/Atx and Plpps and their regulation could bring novel interventional strategies for treating disease.

Accumulative evidence suggests the participation of the ATX-LPA-LPAR axis in skeletal muscles. Yoshida and colleagues provided the first evidence to demonstrate LPA actions in skeletal muscle cells. The authors showed that LPA induced C2C12 myoblast proliferation and cell growth while inhibiting myotube differentiation through Gi proteins (Yoshida et al., 1996). Interestingly, structurally related lipids did not exert the same pro-proliferative and anti-fusion effects as LPA or phosphatidic acid (PA) (Yoshida et al., 1996). Initial evidence suggested the expression of some LPAR genes in skeletal muscle myogenic C2C12 cells in which LPA would activate two known pro-mitogenic signalling pathways, ERK1/2 and AKT (Jean-Baptiste et al., 2005). Other supporting studies have shown that LPA increases intracellular Ca^{2+} concentration and induces DNA synthesis (Xu et al., 2008), reinforcing that LPA modulates myogenic cell growth and proliferation (Bernacchioni et al., 2018). Recently, Ouro and colleagues reported that PA induces DNA synthesis in C2C12 myoblast via LPAR1/LPAR2 and downstream ERK1/2-AKT signalling at similar concentrations of LPA (Gomez-Larrauri et al., 2021), strengthening their mitogenic roles. Pharmacological inhibition of Enpp2/Atx or *Enpp2* knockdown reduces myogenic differentiation, via a mechanism where *Enpp2* is a direct target gene of WNT RSPO2-mediated TCF/LEF/β-Catenin signalling (Sah et al., 2020). The authors also showed that whole-body conditional deletion of *Enpp2* impairs muscle regeneration upon acute $BaCl_2$-induced damage (Sah et al., 2020). Reasoning in favour of a myogenic and pro-regenerative role of Enpp2/Atx, Ray and colleagues recently revealed that the Atx-LPA-Lpar1 axis regulates successful

skeletal muscle regeneration in a satellite cell-specific manner (Ray et al., 2021). Thus, cumulative evidence shows that the ATX-LPA-LPAR-PLPP axis is active in striated muscles modulating muscle stem cell function, adult myogenesis, hypertrophic muscle growth, and regeneration.

Because the exploration of the ATX-LPA-LPAR-PLPP network in muscles has been highly limited to myogenic and satellite cells, there is a current lack of knowledge about the gene expression dynamics of this axis in other muscle cells in response to injury. Here, utilizing publicly available bulk and single-cell transcriptomic datasets, we studied for the first time the gene expression and pathway dynamics of the ATX-LPAR-PLPP network and its changes in numerous cell types in adult muscle homeostasis and regeneration, including subsets immune cells, muscle stem cells, tenocytes, and fibro-adipogenic progenitors.

Results

Skeletal muscle differentially expresses LPAR-ENPP2-PLPP coding genes

To study the LPAR-ENPP2-PLPP pathway's gene expression dynamics in adult skeletal muscle tissue, we utilized public bulk transcriptomic data (Scott et al., 2019) and evaluated LPAR-ENPP2-PLPP gene expression in different samples: whole muscle, lineage^{+} cells (CD31^{+}/CD45^{+}), lineage^{-} cells (CD31^{-}/CD45^{-}), and Lineage^{-}Sca1^{+} FAPs (**Fig. 1A**). In whole muscle tissue, genome-wide transcriptomic profiling shows differential expression of LPAR members. *Lpar1* was the most expressed member, followed by *Lpar6* and *Lpar4*, whereas *Lpar2*, *Lpar3*, and Lpar5 levels were very low (**Fig. 1B**). Limb muscle also expresses *Enpp2* (~8 FPKM) (**Fig. 1B**). Moreover, we evaluated Plpp gene expression dynamics in skeletal muscle tissue. *Plpp1*, *Plpp3*, and *Plpp7* were highly expressed compared to *Plpp2*, *Plpp4*, *Plpp5*, and *Plpp6*. Interestingly, *Lpar6*, *Plpp2*, and *Plpp6* were highly enriched in the lineage+ fraction, suggesting they may be expressed by endothelial or hematopoietic lineage (**Fig. 1A**). Thus, most LPAR-ENPP2-PLPP pathway's components are present in healthy adult skeletal muscle.

Sca1+ fibro-adipogenic progenitors abundantly express LPAR-ENPP2-PLPP coding genes in resting state

Since FAPs have a crucial role in regulating muscle and neuromuscular tissue integrity, we then evaluated the gene expression of the LPAR-ENPP2-PLPP network in muscle-resident Sca1+ FAPs and Hic1+ mesenchymal stromal cells isolated from uninjured muscle tissue (Scott et al., 2019). As observed in skeletal muscle tissue, LPA receptors are differentially expressed in resting FAPs (**Fig. 1C, D**). *Lpar1* is the most expressed family member, followed by *Lpar4* and *Lpar6*, respectively (**Fig. 1C, D**). However, *Lpar2*, *Lpar3*, and *Lpar5* were not significantly expressed in Sca1+ FAPs (**Fig. 1C, D**). These results indicate that *Lpar1* is the highest expressed LPAR member in stromal FAPs, as seen in the fibroblast lineage in other tissues (**Fig. S1**).

FAPs express relatively high levels of *Enpp2* (~77 FPKM) (**Fig. 1E**), suggesting FAPs could be a significant cell source of extracellular LPA. Of the Plpp genes, *Plpp3* was the highest expressed member, followed by *Plpp1* and *Plpp5*. *Plpp2*, *Plpp4*, *Plpp6*, and *Plpp7* genes were very low expressed (**Fig. 1E**). The trend of LPAR-ENPP2-PLPP pathway's gene expression is similar between FAPs and Hic1 expressing cells (**Fig. S2**). These results show that LPAR-ENPP2-PLPP genes are significantly expressed in FAPs and, therefore, suggest a role for the bioactive phospholipid LPA and LPA-mediated signalling in skeletal muscle and stromal progenitor cells in homeostasis.

Analysis of LPAR-ENPP2-PLPP network gene expression in skeletal muscle using single-cell transcriptomics

To gain detailed insights into the role of LPA, its receptors, and Enpp2/Atx-Plpp axis in adult skeletal muscle and muscle cells, we further evaluated the relative expression of LPAR-Enpp2/Atx-Plpp network in skeletal muscle cells using scRNA-seq data (Oprescu et al., 2020). The single-cell data involves uninjured and injured muscle sampled tissues at different time points from early hours post-injury to damage resolution (**Fig. 2A; Fig. S3**). Here, we identified cells with discrete lineage identities and transcriptional states, performing unbiased clustering on an aggregate of cells using the *Seurat* R package (Butler et al., 2018) (**Fig. 2A; Fig. S3**). We initially obtained 29 distinct clusters across different conditions (**Fig. S3A-C**). We visualise distinct cell populations in UMAP dimensionality reduction plots (Materials and methods), representing a total of 19 cell populations and 7 distinct cell lineages (immune cells, tenocytes, fibro-adipogenic progenitors [FAPs] and activated fibroblasts [ActFibroblasts], endothelial cells, pericytes, myonuclei, and muscle stem cells [MuSCs]) across uninjured and injured conditions (**Fig. 2A; Fig. S4**).

Major cell types comprised fibro-adipogenic progenitors (FAPs; Pdgfra+Pi16+Smoc2+Hsd11b1+Cxcl14+), differentiated fibroblasts (DiffFibroblasts; Pdgfra-Meg3+Lum+Col1a1+Dlk1+), muscle stem cells/satellite cells (MuSCs; Cdh15+Pax7+Myog+Megf10+), myonuclei (Ttn+Ckm+Myh1+), pericytes (Rgs5+, which also includes markers of smooth muscle cells i.e., Myh11), endothelial cells (Pecam1+Cdh5+Kdr+Cd36+), tenocytes (Tnmd+Mkx+Fmod+Kera+), Cd8+ T cells (Cd8a+), natural killer T cells (NKTcells; Nkg7), natural killer cells (NKcells; Ccr7+Ccl5+), neutrophils (S100a8+S100a9+Irg1+Tnf+), antigen presenting cells (i.e., B cells, among others) (APCs; H2-Eb1+), dendritic cells (DCs; Cd209a+H2-Eb1+Ccr7+), proliferative immune cells (ProlifICs; Stmn1+Birc5+Mki67+Acp5+), Mrc1 macrophages (Mrc1MO; Mrc1+C1qc+Cx3cr1-Gpnmb-), M1 macrophages (M1MO; Cx3cr1-Pf4+Arg1+Cd36+), monocytes (F10+Chil3+Tnf+), and two related M2 macrophages (M2MO); M2MOCx3cr1hi (C1qc+Cx3cr1^{hi}Tnfaip8l2^{hi}Gpnmb^{low}) and M2MOCx3cr1lo (C1qc+Cx3cr1^{low}Tnfaip8l2^{low}Gpnmb^{hi}) (**Fig. 2A, B; Fig. S4**).

Within the FAP lineage, we observed high transcriptional variation and identified several cluster subtypes with different transcriptomic profiles (**Fig. S3A-C; Fig. S4**). However, for preliminary analysis involving major cell lineages we intentionally grouped 7 main FAP subclusters (clusters 12, 8, 2, 9, 4, 20, and 21) and kept differentiated fibroblasts (DiffFibroblasts, cluster 15) aside (**Fig. 2A, B; Fig. S3; Fig. S4**). DiffFibroblasts have a differentiated fibroblasts/myofibroblast-like gene signature, highly expressing markers of activation and differentiation or loss of stemness (Pdgfra-Pi16-Lum+Col1a1+Dlk1+Col3a1+Col6a3+) (**Fig. 2B; Fig. S4**). Downregulation of *Pdgfra* is sign of a differentiated FAP phenotype and corresponds to their loss of stemness (Contreras et al., 2019, 2020; Soliman et al., 2020).

Our analysis shows that fibro-adipogenic progenitors, tenocytes, and satellite cells, predominantly express *Lpar1*, but its expression was higher in tenocytes and FAPs than MuSCs (**Fig. 2C, D**). Remarkably, *Lpar1* expression has not been previously shown in tenocytes or FAPs, although it has been described that myogenic and MuSCs express functional LPAR1 (Ray et al., 2021). *Lpar4* was expressed in FAPs but not highly expressed in other cell types (**Fig. 2C, D**). *Lpar2*, *Lpar3*, and *Lpar5* genes are virtually absent in FAPs (**Fig. 2C, D**), which corroborates our previous results exploring bulk RNAseq data of Sca1+ FAPs (**Fig. 1D**). On the contrary, *Lpar6* has a broader cell type-dependent expression, expressed by different populations of immune cells (e.g., monocytes and APCs) and endothelial cells (**Fig. 2C, D**). Interestingly, *Lpar6* is the only LPAR member expressed in the immune cell lineage, suggesting that LPA or related phospholipids may also modulate immune cell function. These findings better define the bulk RNAseq analyses shown in **Figure 1** for lineage^{+} cells.

On the other hand, FAPs and tenocytes express high levels of Enpp2/Atx, which was barely detected in other cell types (**Fig. 2C, D**). This suggests FAPs and tenocytes as the two major cell types responsible for extracellular LPA production in skeletal muscles. With relation to LPA catabolizing enzymes, FAPs highly express *Plpp1*, followed by *Plpp3* and *Plpp5* (**Fig. 2C, D**). MuSCs express *Plpp1* and *Plpp2* but no other members, whereas pericytes only *Plpp3* (**Fig. 2C, D**). Endothelial cells highly express *Plpp3* gene and, to a lesser degree, *Plpp1* (**Fig. 2C, D**). Tenocytes also highly express *Plpp3* and *Plpp1*, and less of *Plpp5* (**Fig. 2C, D**). M2-like Mrc1+ macrophages specifically express *Plpp3*. Myonuclei only express *Plpp7* (**Fig. 2C, D**). Intriguingly, we could not detect *Plpp4* in the analyzed data, which could be due to the very low expression of this *Plpp* gene as seen before exploring bulk RNAseq (**Fig. 1**). Hence, our analysis reveals for the first time a detailed landscape of Lpar-Enpp2/Atx-Plpp gene expression in several muscle cells in homeostasis and regeneration at single-cell resolution, suggesting an active role of FAPs and tenocytes in producing LPA.

Analysis of Lpar-Enpp2/Atx-Plpp axis expression in fibro-adipogenic progenitor subpopulations in response to skeletal muscle regeneration

Fibro-adipogenic progenitors and lineage are the primary cell type responsible for ectopic fibrosis, fatty tissue, and bone formation and deposition in severe myopathies, degenerative disorders, and neuromuscular disease (Contreras et al., 2021). Thus, we explored the temporal gene expression dynamics of Lpar-Enpp2/Atx-Plpp members in FAPs in homeostasis and in response to acute damage. We performed unbiased clustering on an aggregate of the initial clusters number 12, 8, 2, 9, 4, 20, and 21 (**Fig. S3**). We decided to include tenocytes (initial cluster 17 (**Fig. S3; Fig. S4**)) in our clustering analysis since these cells share a mesenchymal origin and highly express *Lpar1* and *Enpp2*/Atx.

Our unbiased subcluster analysis retrieved 10 distinct clusters (**Fig. 3A**). Using *FindAllMarkers* Seurat function in these clusters and determining the top 8 marker genes, we assigned different names for the eight FAP subtypes obtained and labelled tenocytes (**Fig. 3B, C**). On the other hand, all FAP subpopulations showed expression of canonical FAP markers *Pdgfra* and *Sparcl1*, albeit at varying proportions and levels (**Fig. S5A-C**), and major changes in cell proportions were seen between conditions or days of injury (**Fig. 3D, E**). We named these cells Sparcl1 FAPs, Csrp2 FAPs, Dlk1 FAPs, Dpp4 FAPs, Hsd11b1 FAPs, Tyrobp FAPs (previously named as DiffFibroblasts), Cycling FAPs, and Ccl2 FAPs, starting from the most numerous subpopulations of FAPs to the less abundant (**Fig. 3B, C**). We also observed noticeable transcriptomic changes in the top 8 expressed genes following muscle injury (**Fig. 3D**). The top 8 expressing genes of Sparcl1 FAPs are *Sparcl1*, *Abca8a*, *Col15a1*, *Hmcn2*, *Htra3*, *Ltbp4*, *Penk*, and *Cfh* (**Fig. 3E**). Csrp2 FAPs highly express *Csrp2*, *Sfrp2*, *Ltbp2*, *Lrrc15*, *Tnc*, *1500015O10Rik*, *Acta2*, and Tagln, whereas Dlk1 FAPs were highly expressing *Dlk1*, *Igf2*, *Plagl1*, *Mest*, *Zim1*, *H19*, *Nrk*, and *Agtr2*. Dpp4 FAPs top 8 expressed genes are *Efhd1*, *Pcolce2*, *Dpp4*, *Sema3c*, *Cd55*, *Pi16*, *Efemp1*, and *Stmn4*. *Hsd11b1*, *Ccl11*, *Crispld2*, *Vwa1*, *Enpp2*, *G0s2*, *Nmb*, and *Inmt* genes characterized Hsd11b1 FAPs between other FAP subtypes, although these also highly express *Cxcl14* (**Fig. 3E**). Tyrobp FAPs express *Tyrobp*, *Fcer1g*, *Ctss*, *Lyz2*, *Laptm5*, *Slfn2*, *Cd52*, *Srgn*, whereas Cycling FAPs were characterized by highly expressing genes related to survival and cell cycle, including *2810417H14Rik*, *Stmn1*, *Birc5*, *Mki67*, *Cks2*, *Tpx2*, *Cenpa*, and *Top2a*. Finally, Ccl2 FAPs high express *Cxcl5*, *Ddx21*, *Ccl2*, *Rdh10*, *Slco2a1*, *Prg4*, *Lif*, and *Mmp3*, highlighting a pro-inflammatory state of these cells at 12 hours post-injury (**Fig. 3E**). The tenocyte cluster highly expresses *Tnmd*, *Fmod*, *Thbs4*, *Col11a1*, *Cilp2*, *Scx*, *Kera*, and *Chodl*, as previously described (Harvey et al., 2019; Scott et al., 2019).

In uninjured conditions, we could distinguish two distinct FAP populations based on scRNA-seq. We termed these Hsd11b1 FAPs, and Dpp4 FAPs as the highest upregulated gene in Hsd11b1 FAPs was *Hsd11b1,* and Dpp4 FAPs highly expressed *Dpp4* (**Fig. 3A-E; Fig. S5**), as previously described (Scott et al., 2019; Oprescu et al., 2020). Earlier in the injury process, Ccl2 FAPs relate to an activated immune-like pro-inflammatory FAP subpopulation mostly present at 12 hours post-injury (**Fig. 3A-B**). Cycling FAPs uniquely expressed a potent cell cycle gene signature, representing the most abundant FAP subtype found at 2 days post-injury (**Fig. 3A-E; Fig. S5**). Cycling FAPs can also be found at 3.5- and 5-days post-injury but to a lesser extent (**Fig. 3A-E; Fig. S5**). Csrp2 FAPs are more abundant at 3.5- and 5-days post-injury, whereas Dlk1 FAPs at 10 days (**Fig. 3A-E; Fig. S5**). The final captured stage of skeletal muscle regeneration, corresponding to day 21, mostly identifies Sparcl1 FAPs together with Tyrobp FAPs (corresponding to DiffFibroblasts in our initial clustering) and, to a lesser extent, some Dpp4 FAPs (**Fig. 3A-E; Fig. S5**).

Next, we further identified the expression profiles of the Lpar-Enpp2/Atx-Plpp axis in the different FAP subpopulations. Most major FAP subtypes express *Lpar1*, including Dpp4, Dlk1, and Sparcl1 FAPs at high levels (**Fig. 3F, G**). *Lpar1* was also expressed in Hsd11b1, Csrp2, Ccl2, and Cycling FAPs, although to a lesser extent (**Fig. 3F, G**). *Lpar1* is also highly expressed by tenocytes (**Fig. 3F, G**). Noticeable, *Lpar1* gene expression was deficient in Tyrobp FAPs compared to the other 7 FAPs subtypes, suggesting Lpar1-dependent signalling may be downregulated in day 21 differentiated fibroblasts-like FAPs (**Fig. 3F, G**). No significant gene expression was detected for *Lpar2*, *Lpar3*, *Lpar5*, and *Lpar6* in FAPs or tenocytes (**Fig. 3F, G**). *Lpar4* was primarily expressed in Dlk1 and Sparcl1 and to a less extent in uninjured Hsd11b1 FAPs and Dpp4 FAPs (**Fig. 3F, G**). These results show that different FAP subpopulations that exist in homeostasis and others that appear following acute damage express different levels of LPA receptors, suggesting LPA may modulate FAP activation, survival, and fate primarily throughout LPAR1 and LPAR4. Also, the absence of LPA receptors' gene expression in the Tyrobp FAPs subtype compared to their existent counterparts at day 21 (e.g., Sparcl1 and Dpp4 FAPs) suggests Tyrobp FAPs may be refractory to LPA actions (**Fig. 3E-G**). Thus, our single-cell exploration reports highly dynamic gene expression of LPA receptors in fibro-adipogenic progenitors in homeostasis and skeletal muscle regeneration.

Enpp2 (Atx) gene expression was higher in uninjured Hsd11b1 FAPs and Dpp4 FAPs than Sparcl1, whereas repressed in other FAP subpopulations (**Fig. 3E-G**). Remarkably, Enpp2/Atx gene expression was among the top 5 markers expressed in Hsd11b1 FAPs (**Fig. 3C, E**). Dpp4 FAPs also highly express *Enpp2*/Atx (**Fig. 3C-G**), suggesting a role for the LPA extracellular-producing enzyme in resting FAPs, yet to be discovered. Tenocytes express *Enpp2* at levels comparable to Sparcl1 FAPs (**Fig. 3E-G**). Among Plpp genes, *Plpp3* gene expression was the most broadly distributed (Fig. 3E-G), although its expression was higher in Dpp4 FAPs, followed by Hsd11b1 and Sparcl1 FAPs but downregulated in other FAP subpopulations (**Fig. 3E-G**). On the contrary, *Plpp1* and *Plpp5* gene expression patterns were similar, except for Ccl2 FAPs that did not express *Plpp5* but *Plpp3* (**Fig. 3E-G**). Among Plpp genes, Tyrobp FAPs only expressed one family member *Plpp3* (**Fig. 3E-G**) As previously suggested, *Plpp2*, *Plpp6*, and *Plpp7* genes were absent in most FAP subtypes, with a small percent of Ccl2 FAPs expressing *Plpp2* and Hsd11b1 FAPs expressing *Plpp7* (**Fig. 3E-G**). Thus, our single-cell transcriptomic analyses show enrichment of the extracellular LPA-producing enzyme Enpp2/Atx in two FAP subpopulations Hsd11b1 and Dpp4, suggesting resting FAPs as a significant source of LPA in homeostatic and regenerated skeletal muscles.

Downregulation of LPA receptors in fibro-adipogenic progenitors in response to acute injury

To better understand the single-cell gene expression patterns of the LPA receptor family in adult FAPs during muscle regeneration, we grouped all FAP clusters. We then evaluated *Lpar* gene expression in response to injury (**Fig. S5E**). Skeletal muscle injury triggers a rapid and pronounced downregulation of LPA receptors in FAPs, including *Lpar1*, *Lpar4*, and *Lpar6* (**Fig. 4A; Fig. S5E**). *Lpar1*, *Lpar4*, and *Lpar6* gene expression is drastically downregulated at 12 h and stays low up to 48 h post-muscle injury (**Fig. 4A; Fig. S5E**). Then, their gene expression increases and recovers from 3.5 days to 10 days post-injury (**Fig. 4A**). Remarkably, *Lpar1* and *Lpar4* were upregulated later, day 21 (**Fig. 4A**). Since these changes happen when FAPs activate and commit to proliferate and expand their numbers (**Fig. 3; Fig. S5D**), they suggest an association between FAP activation and cell cycle dynamics with expression repression of LPAR family members. Finally, we determined the relative gene expression of LPA receptors at the genome-wide transcript level in quiescent and injury-activated tdTomato Hic1 expressing mesenchymal stromal cells in muscle (Scott et al., 2019) (**Fig. 4B, C**). *Lpar1* was highly and preferentially expressed over *Lpar4* and *Lpar6* in quiescent and injury-activated Hic1 expressing mesenchymal stromal cells (MSCs) (**Fig. 4B, C**). *Lpar2*, *Lpar3*, and *Lpar5* were low expressed (**Fig. 4B, C**). *Lpar1* gene expression was early repressed in MSCs following acute damage, reaching its lowest on day 3 but recovering from day 4 post-injury onwards. Hence, two independent datasets demonstrate that the expression of the LPAR family members is dynamically downregulated in injury activated FAPs and MSCs, but it recovers later as muscle damage resolves through regeneration.

Repression of Enpp2/Atx and Plpp genes in fibro-adipogenic progenitors in response to acute injury

Next, we evaluated Enpp2/Atx expression in Hic1+ MSCs. *Enpp2* was highly expressed in quiescent Hic1 tdTomato+ cells but dramatically downregulated 1-day post-injury, then increasing halfway through up to day 3 to being reduced again until day 5 post-acute muscle injury (**Fig. 5A; Fig. S5E**). *Enpp2* expression goes up from day 5 to day 10 post-injury (**Fig. 5A**). At single-cell resolution, *Enpp2* shows a similar expression pattern in FAPs to that of Hic1 expressing cells (**Fig. 5A, B**), which is expected since Hic1 expressing cells mainly comprise FAPs in adult skeletal muscles (Scott et al., 2019; Contreras, 2020). Hence, *Enpp2* is drastically downregulated to almost undetectable levels in FAPs at regenerative time points that associate with cell activation and proliferation (**Fig. S5D, E**). *Enpp2* levels in FAPs remained very low up to 5 days, then recovering from day 10 to day 21 post-injury (**Fig. 5B; Fig. S5E**).

Hic1 expressing cells repress *Plpp3* gene expression following injury, whereas *Plpp1* and *Plpp5* transiently increased (**Fig. 5C**). These changes are contrasted by our single cell results in FAPs. *Plpp* genes are significantly downregulated early while its expression recovered at later regenerative time points in FAPs at single cell level (**Fig. 5E**). These results highlight the initial intense

downregulation of the enzyme that produces extracellular LPA, while different *Plpp* genes followed a similar pattern of repression.

Upregulation of *Lpar1* and *Lpar4* associates with an activated muscle stem cell state

Rai and colleagues recently reported that Atx-LPA-LPAR1 signalling is a crucial pro-regenerative axis in skeletal muscle (Ray et al., 2021). The authors also showed that Lpar1 expression increased in myotubes compared to proliferative myoblasts, suggesting a pivotal role of LPA in modulating adult satellite cell function.

To better understand the single-cell gene expression dynamics of the LPAR family in adult MuSCs, we again used scRNA-seq data and performed unsupervised subclustering on the MuSC metacluster, as previously shown (Oprescu et al., 2020; Contreras et al., 2021a). Six different subsets of MuSCs resulted from our analysis, consistent with previous findings (Oprescu et al., 2020; Contreras et al., 2021a) (**Fig. S6A**). Quiescent (QSC) adult MuSCs express *Lpar1* and *Lpar4* but no other LPAR members (**Fig. 6A, Fig. S6B**). *Lpar1* and *Lpar4* remain relatively stable in activated MuSCs (ASC) to decrease in dividing (DIV), committed (COM), immunomyoblasts (IMB) and differentiated (DIF) MuSCs (**Fig. 6A, Fig. S6B**), suggesting both LPA receptors are downregulated as muscle stem cells commit and differentiate to form mature myofibers.

Among the phospholipid phosphatases expressed in quiescent MuSCs, *Plpp3* was the most expressed member of the family and its expression progressively decreased as these cells activated, committed, and differentiated (**Fig. 6B; Fig. S6B**). *Plpp1* was significantly higher in activated, committed, and differentiating MuSCs, whereas *Plpp2* increased only in immunomyoblasts, activated, and dividing MuSCs (**Fig. 6B; Fig. S6B**). *Plpp5* and *Plpp6* were not considerably expressed in MuSCs (**Fig. 6B; Fig. S6B**). The non-enzymatic member, *Plpp7*, was absent in each of the six MuSCs subpopulations except in differentiated MuSCs (**Fig. 6B; Fig. S6B**). Surprisingly, just a few percent of quiescent MuSC express *Enpp2* (**Fig. S6B**). *Enpp2* expression further decreased in ASC, DIV, IMB, COM, and DIF MuSCs subpopulations (**Fig. 6C; Fig. S6B**). Thus, our results show that Enpp2/Atx levels are confined to just a small subset of MuSCs, but functional data from Ray et al show that this is sufficient to have biological relevance. These single cell transcriptomic analyses suggest that the expression of LPAR-Atx-Plpp is dynamic in muscle stem cells in homeostasis and injury. They also illustrate the potentially complex cell communication networks mediated by the bioactive phospholipid LPA in skeletal muscle and the MuSC niche.

Discussion

LPA is a signalling lipid with multiple biological functions and roles in health and disease. Our results support the presence of the ATX-LPAR-PLPP axis in different muscle cells, tendon cells, and FAP lineage in homeostasis and injury, providing a detailed view of the temporal transcriptomic dynamics of the ATX-LPAR-PLPP axis during skeletal muscle regeneration at single cell resolution. We first showed that different skeletal muscle cells differentially express Lpar-Enpp2-Plpp protein-coding genes. *Lpar1* is the highest expressed member among other LPARs, followed by *Lpar6* and *Lpar4*. We also found that *Lpar2*, *Lpar3*, and *Lpar5* were almost unexpressed. Autotaxin (*Enpp2*) is a relatively abundant gene in *tibialis anterior* limb muscle, and several Plpp were also expressed, including *Plpp1*, *Plpp3*, and *Plpp7*. Thus, we report most LPAR-Enpp2-Plpp pathway's components are present in healthy adult skeletal muscle in mice. Remarkably, two stromal cell types, including tenocytes and FAPs, highly express *Lpar1* and Enpp2/Atx, suggesting stromal cells may be the primary source of extracellular LPA and LPA-mediated signalling and functions in the muscle niche.

By subclustering stromal fibro-adipogenic progenitors (FAPs), we identified different populations representing distinct cell states with robust LPAR and Enpp2/ATX transcriptome signatures in homeostasis. *Lpar1* was expressed mainly by different subset of FAPs and tenocytes, whereas Enpp2/Atx was mostly expressed by resting FAPs. We also show that tissue injury induces strong and fast repression of LPA receptors and Enpp2/Atx. Uniquely activated FAP cell states are partly defined by a strong downregulation of *Lpar*-Enpp2/Atx gene expression. Hence, our data analysis highlights LPA-LPAR-ENPP2-PLPP in different muscle cells and fibro-adipogenic progenitor lineages after muscle injury and provides an entry point for more profound research of the role of LPA signalling in homeostasis, inflammation, fibrosis, repair, and regeneration. Finally, focusing on different MuSCs subtypes that emerge following acute damage we also observed differential LPAR-ENPP2-PLPP axis gene expression, although in general terms the axis was low expressed compared to FAPs and tenocytes. Activated muscle stem cell state associates with *Lpar1* and *Lpar4* upregulation, suggesting as satellite cells abandon their resting state, they would increase the expression of LPARs, which in turn could bind niche-stored or damaged-released LPA increasing the responsiveness of satellite cell lineage cells to local LPA.

Ray and colleagues recently showed that myogenic differentiation induces Atx expression, increasing its extracellular abundance, and Atx knockdown reduced fusion and myotube differentiation (Ray et al., 2021). Remarkably, the cell-specific deletion of Atx in MuSCs impairs acute injury-induced muscle regeneration in mice, resulting in reduced muscle fiber caliber (Ray et al., 2021). These results were supported by utilizing a pharmacological Atx inhibitor, which also caused reduced muscle regeneration. Furthermore, Atx transgenic mice overexpressing circulating and extracellular Atx levels, and expectedly increasing serum LPA, showed signs of muscle hypertrophy via ribosomal S5K

signalling and accelerated recovery post-acute damage (i.e., faster muscle regeneration) (Ray et al., 2021). In support of this, intramuscular injections of both Atx and LPA into healthy muscles resulted in muscle hypertrophy. These results provide significant data in favour of a pro-regenerative role of the ATX-LPA-LPAR axis in skeletal muscles. On the other hand, Kienesberger and colleagues showed that the ATX-LPA axis is involved in obesity-induced insulin resistance in muscles, affecting mitochondrial respiration in differentiated myotubes (D'Souza et al., 2018), validating the previously suggested key role of ATX-LPA axis in healthy and obese adipose tissue (Ferry et al., 2003; Boucher et al., 2005; Federico et al., 2012). The authors also showed that partial genetic reduction of ATX ameliorated obesity and systemic insulin resistance in a high-fat diet mouse model (D'Souza et al., 2018). These results suggest that the ATX-LPA axis could contribute to the development of obesity-related disorders and tissue malfunction in metabolically altered states.

We and others have demonstrated that LPA induces the gene expression and protein levels of biologically active Connective Tissue Growth Factor (CTGF/CCN2) in C2C12 myoblasts (Vial et al., 2008; Riquelme-Guzmán et al., 2018). CTGF/CCN2 is a matricellular regulatory protein that modulates skeletal muscle repair, muscular dystrophy pathophysiology, and fibrosis (Morales et al., 2013; Petrosino et al., 2018, 2019; Rebolledo et al., 2019; Chen et al., 2020). LPA-mediated CTGF/CCN2 induction has been reported in different cell types, including embryonic and adult fibroblasts, mesothelial cells, in human and mouse models (Heusinger-Ribeiro et al., 2001; stortelers et al., 2008; Sakai et al., 2013). Remarkably, several ubiquitous signalling pathways mediate LPA-mediated CTGF/CCN2 induction in myogenic cells, including αvβ3 and αvβ5 Integrins, TGF-b receptor kinase activity, JNK, ECM components, and FAK (Cabello-Verrugio et al., 2011; Riquelme-Guzmán et al., 2018). These studies reveal an intricated network of signalling molecules that may tune LPA-driven responses in cells and tissues. Remarkably, Chen and colleagues showed that LPA, which has been previously identified to increase upon myocardial infarction (Chen et al., 2003), promote proliferation and apoptosis of cardiac fibroblasts depending on its concentrations, suggesting that LPA has dual roles in fibroblasts (Chen et al., 2006).

Recently, Brandan and colleagues showed that intramuscular injections of LPA induced CTGF/CCN2 protein levels and few ECM proteins (Córdova-Casanova et al., 2022). Using LPAR inhibitor Ki16425 or LPAR1 knockout mice the authors observed an inhibition of these effects. They also showed increase muscle cellularity (i.g., total number of nuclei) and number of PDGFRa+ FAPs in response to LPA intramuscular injections. These results indicate LPA could have fibrotic-like properties *in vivo* in damaged muscles as previously suggested using cell culture (Vial et al., 2008; Riquelme-Guzmán et al., 2018) or *in vivo* models (Davies et al., 2017).

Periodic intraperitoneal injections of LPA worsen the inflammatory milieu of rotator cuff tears (RCTs) in adult rats, increasing *Tnfa* and *Tgfb1* at six weeks post tear and the number of inflammatory

cells within the affected muscles (Davies et al., 2017). Rotator cuff tears (RCTs) are a highly prevalent form of muscle trauma and tissue degeneration (Agha et al., 2021). Since severe intramuscular fibrosis and fatty infiltration are key morphological features of RCTs, significant research suggests FAPs as critical mediators of RCT onset, pathology, and progression (Theret et al., 2021). The authors also showed that enhanced systemic LPA worsens the fibrotic and adipogenic phenotype of RCTs (Davies et al., 2017). Thus, this is the first study of its kind to demonstrate a pro-fibrotic and pro-adipogenic role of systemic LPA in damaged muscles. Since FAPs are the main mediators of ectopic fibrous and fatty tissue, and because our results show resting FAPs highly express LPAR1 and Enpp2/Atx, we speculate that LPA acts on these stromal cells early after muscle injury to promote cell proliferation and survival, and therefore, resulting in a fibrotic and adipogenic phenotype in severely damaged muscles. However, the role of LPA in modulating the fate and differentiation of muscle-resident FAPs has not been explored yet. Although forced intramuscular injections with LPA may not reflect proper physiological or pathophysiological conditions, the results of Córdova-Casanova et al. together with those of Davis et al., offer a new avenue to start exploring the relevance of LPA-mediated signalling pathways and their role in muscle disease and physio-pathophysiology.

Due our analysis also showed that endothelial cells and several immune cell types, including monocytes, M2Cxc3cr1^{hi} macrophages, and APCs express *Lpar6*, we could also consider that intramuscular or intraperitoneal injections of LPA target endothelial and immune cells. In this regard, LPA promotes the development of macrophages from monocytes through a mechanism that may involve PPARγ (Ray and Rai, 2017). Hence, our results suggest that injury-induced LPA could act on monocyte to promote their maturation and differentiation into macrophages via Lpar6.

Despite the involvement of the LPA-LPAR-ATX axis in inflammation and fibrosis development is not new but several well-supported studies have shown its crucial participation (Tager et al., 2008; Castelino et al., 2011; Gan et al., 2011; Sakai et al., 2013; Ohashi and Yamamoto, 2015; He et al., 2018; Ninou et al., 2018), the mechanisms and cellular targets have been underexplored. Several ongoing studies suggest the LPA-LPAR-ATX as a prognostic indicator of injury- or radiation-induced fibrosis (NCT05031065), with some studying or studied the safety, tolerance, and effectiveness of orally available Atx inhibitors (BBT-877: NCT03830125; GLPG1690 (ziritaxestat): NCT02738801 and NCT03798366) or LPAR antagonists (BMS-986020: NCT01766817 (Decato et al., 2022); BMS-986278: NCT04308681), as meanings of reducing tissue fibrosis and improving organ function in different patients cohorts. Because stromal cells of mesenchymal origin (e.g., FAPs and tenocytes) highly express Lpar-Enpp2/Atx-Plpp members, upcoming research should focus in better understanding the role of LPA axis in muscle homeostasis, inflammation, fibrosis, repair, and regeneration. This understanding would potentially offer new druggable avenues for devastating muscle diseases like myopathies, severe muscle trauma, or neuromuscular disorders.

Hence, applying bulk and single cell transcriptomic data analyses we zoom in on skeletal muscle tissue at single cell resolution and provide for the first time a detailed view of the LPA-LPAR-Enpp2/Atx-PLPP axis for future insights in how to target LPA-driven signalling and functions.

Limitations of the study

This study has certain inherent limitations. First, our transcriptomics analyses cannot address the protein levels of the ATX-LPA-LPAR-PLPP network; however, there is a limitation of validated and working antibodies of the axis' components to date. Second, we have not evaluated or measured the effects of exogenous LPA on modulating the fate of immune, MuSCs, tenocytes, endothelial cells, or fibro-adipogenic progenitors. More subsequent studies should focus on understanding the influence and role of the ATX-LPA-LPAR-PLPP network and its effects on the fate of different muscle cells. Third, although we detected a strong and fast downregulation of LPARs in FAPs in response to injury, we did not evaluate LPA receptor protein levels in FAPs upon injury-induced activation. The development of high-quality and validated LPAR antibodies should help answer these and other related questions. Fourth, commonly used tissue disaggregation strategies, flow cytometry, and droplet-based scRNAseq does not efficiently capture certain cell types (e.g., adipocytes) because of their high propensity to rupture and buoyancy. On top of that, large cells (e.g., myofibers, nerves, and adipocytes) do not effectively fit into a droplet and are often underrepresented in scRNAseq studies. Nevertheless, our study represents the first of its kind since it explores the ATX-LPA-LPAR-PLPP network at single-cell resolution. Thus, our bulk and single-cell transcriptomic explorations aim to add solid and cumulative evidence to the emerging field of ATX-LPA-LPAR-PLPP axis in muscles and regeneration and unveil yet-to-be-discovered novel roles of it in other organs and contexts.

Materials and methods

scRNA-seq data processing and analyses

We extracted the single-cell RNA sequencing data used in this paper from Gene Expression Omnibus (GEO; GSE138826) (https://www.ncbi.nlm.nih.gov/geo/query/acc.cgi?acc=GSE138826; GSE138826_expression_matrix.txt) (Oprescu et al., 2020). The preliminary analyses of processed scRNA-seq data were analysed using the Seurat suite (version 4.0.3) standard workflow in RStudio Version 1.2.5042 and R version 4.0.3. First, we applied initial quality control to Oprescu et al., 2020 dataset. We kept all the features (genes) expressed at least in 5 cells and cells with more than 200 genes detected. Otherwise, we filtered out the cells. Second, we verified nUMIs_RNA (> 200 & < 4000) and percent.mt. (less than 5%) Third, UMIs were normalized to counts-per-ten-thousand log-transformed (normalization.method = LogNormalize). The log-normalized data were then used to find variable genes (*FindVariableFeatures*) and scaled (*ScaleData*). Finally, *Principal Component Analysis* (PCA) was run (*RunPCA*) on the scaled data using highly variable features or genes. *Elbowplot* were used to decide the number of principal components (PCs) to use for unsupervised graph-based clustering and dimensional reduction plot (UMAP) embedding of all cells or further subclustering analyses (i.e., FAPs) using the standard *FindNeighbors*, *FindClusters*, and *RunUMAP* workflow. We used 30 PCs and a resolution of 0.6 to visualize a Uniform manifold approximation and projection (UMAP) dimensionality reduction plot generated on the same set of PCs used for clustering. We decided the resolution value for FindClusters on a supervised basis after considering clustering output from a range of resolutions (0.4, 0.6, 0.8, and 1.2). We used a resolution of 0.6. Our initial clustering analysis returned 29 clusters (clusters 0-28). We identified cell populations and lineage-specific marker genes for the analysed dataset using the *FindAllMarkers* function with logfc.threshold = 0.25, test.use = “wilcox”, and max.cells.per.ident = 1000. We then plotted the top 10 expressed genes, grouped by orig.ident and seurat_clusters using the *DoHeatmap* function. We determine cell lineages and cell types based on the expression of canonical genes. We also inspected the clusters (in Figure 2 and Figure 3) for hybrid or not well-defined gene expression signatures. Clusters that had similar canonical marker gene expression patterns were merged.

For Mesenchymal Clusters (group of FAPs + DiffFibroblasts + Tenocytes obtained in **Figure 2**) we used PCs 20 and a resolution of 20 to visualize on the UMAP plot. Our mesenchymal subclustering analysis returned 10 clusters (clusters 0-9). Cell populations and lineage-specific marker genes were identified for the analysed dataset using the *FindAllMarkers* function with logfc.threshold = 0.25 and and max.cells.per.ident = 1000. We then plotted the top 8 expressed genes, grouped by orig.ident and seurat_clusters using the *DoHeatmap* function. The identity of the returned cell clusters was then annotated based on known marker genes (see details about cell type and cell lineage definitions in the main text, results section). Individual cell clusters were grouped to represent cell

lineages and types better. Finally, figures were generated using *Seurat* and *ggplot2* R packages. We also used dot plots because they reveal gross differences in expression patterns across different cell types and highlight moderately or highly expressed genes.

The scRNAseq pipeline used for MuSC subclustering was developed following previous studies (Oprescu et al., 2020; Contreras et al., 2021a). To perform unsupervised MuSC subclustering, we used Seurat's subset function *FindClusters*, followed by dimensionality reduction and UMAP visualization (*DimPlot*) in Seurat.

Bulk RNA-seq data processing and analyses

We generated the heat maps shown in Figure 1 and Figure 2 with Morpheus (https://software.broadinstitute.org/morpheus/) using previous transcriptomic available RNA-seq data extracted from GEO (GSE110038) (Scott et al., 2019).

Statistical analysis

Mean±s.e.m. values, as well as the number of experiments performed, are indicated in each figure. Bulk RNAseq data were collected in Microsoft Excel, and statistical analyses were performed using GraphPad Prism 9.4.0 software for macOS Monterey. All bulk RNAseq datasets used to determine gene expression were analyzed for normal distribution using the Shapiro-Wilk test with a significant level set at alpha = 0.05. Statistical significance of the differences between the means was evaluated using the One-Way ANOVA test followed by post-hoc Dunnett or Tukey's multiple comparisons tests, and the significance level was set at $P < 0.05$ (95% confidence interval). *P*-value style: GP: 0.0332 (*), 0.0021 (**), 0.0002 (***), < 0.00001 (****).

Data accessibility

This article has no additional data. Software used to analyze the data freely or commercially available.

CRediT Author Contribution

Osvaldo Contreras: Conceptualization, Data curation, Formal Analysis, Investigation, Methodology, Project administration, Resources, Software, Supervision, Validation, Visualization, Writing – original draft, Writing – review & editing. Osvaldo Contreras gave final approval for publication and agreed to be held accountable for the work performed therein.

Funding

Osvaldo Contreras did not receive specific funding to develop this work.

Competing interests

The author declares that the research was conducted in the absence of any commercial or financial relationships that could be construed as a potential conflict of interest.

Acknowledgements

I would like to thank Drs Yen Tran, Qing Wang, and Camilo Riquelme-Guzman for their help proofreading this manuscript. O.C. is an investigator of the Victor Chang Cardiac Research Institute and the University of New South Wales.

References

Agha, O., Diaz, A., Davies, M., Kim, H. T., Liu, X., and Feeley, B. T. (2021). Rotator cuff tear degeneration and the role of fibro-adipogenic progenitors. *Ann. N. Y. Acad. Sci.* 1490, 13–28. doi:https://doi.org/10.1111/nyas.14437.

Akira, T., Kengo, H., Kenji, F., and Hiroaki, T. (1986). Involvement of lysophospholipase D in the production of lysophosphatidic acid in rat plasma. *Biochim. Biophys. Acta - Lipids Lipid Metab.* 875, 31–38. doi:https://doi.org/10.1016/0005-2760(86)90007-X.

Baghdadi, M. B., and Tajbakhsh, S. (2018). Regulation and phylogeny of skeletal muscle regeneration. *Dev. Biol.* 433, 200–209. doi:https://doi.org/10.1016/j.ydbio.2017.07.026.

Benesch, M. G. K., Zhao, Y. Y., Curtis, J. M., McMullen, T. W., and Brindley, D. N. (2015). Regulation of autotaxin expression and secretion by lysophosphatidate and sphingosine 1-phosphate. *J. Lipid Res.* 56, 1134–1144. doi:https://doi.org/10.1194/jlr.M057661.

Bernacchioni, C., Cencetti, F., Ouro, A., Bruno, M., Gomez-Muñoz, A., Donati, C., et al. (2018). Lysophosphatidic Acid Signaling Axis Mediates Ceramide 1-Phosphate-Induced Proliferation of C2C12 Myoblasts. *Int. J. Mol. Sci.* 19. doi:10.3390/ijms19010139.

Binder, B. Y. K., Williams, P. A., Silva, E. A., and Leach, J. K. (2015). Lysophosphatidic Acid and Sphingosine-1-Phosphate: A Concise Review of Biological Function and Applications for Tissue Engineering. *Tissue Eng. Part B Rev.* 21, 531–542. doi:10.1089/ten.teb.2015.0107.

Boucher, J., Quilliot, D., Pradères, J. P., Simon, M. F., Grès, S., Guigné, C., et al. (2005). Potential involvement of adipocyte insulin resistance in obesity-associated up-regulation of adipocyte lysophospholipase D/autotaxin expression. *Diabetologia* 48, 569–577. doi:10.1007/s00125-004-1660-8.

Brindley, D. N., Pilquil, C., Sariahmetoglu, M., and Reue, K. (2009). Phosphatidate degradation: Phosphatidate phosphatases (lipins) and lipid phosphate phosphatases. *Biochim. Biophys. Acta - Mol. Cell Biol. Lipids* 1791, 956–961. doi:https://doi.org/10.1016/j.bbalip.2009.02.007.

Butler, A., Hoffman, P., Smibert, P., Papalexi, E., and Satija, R. (2018). Integrating single-cell transcriptomic data across different conditions, technologies, and species. *Nat. Biotechnol.* 36, 411. Available at: https://doi.org/10.1038/nbt.4096.

Cabello-Verrugio, C., Córdova, G., Vial, C., Zúñiga, L. M., and Brandan, E. (2011). Connective tissue growth factor induction by lysophosphatidic acid requires transactivation of transforming growth factor type β receptors and the JNK pathway. *Cell. Signal.* 23, 449–457. doi:10.1016/j.cellsig.2010.10.019.

Castelino, F. V, Seiders, J., Bain, G., Brooks, S. F., King, C. D., Swaney, J. S., et al. (2011). Amelioration of dermal fibrosis by genetic deletion or pharmacologic antagonism of lysophosphatidic acid receptor 1 in a mouse model of scleroderma. *Arthritis Rheum.* 63, 1405–1415. doi:https://doi.org/10.1002/art.30262.

Chen, J., Han, Y., Zhu, W., Ma, R., Han, B., Cong, X., et al. (2006). Specific receptor subtype mediation of LPA-induced dual effects in cardiac fibroblasts. *FEBS Lett.* 580, 4737–4745. doi:https://doi.org/10.1016/j.febslet.2006.07.061.

Chen, X., Yang, X. Y., Wang, N. D., Ding, C., Yang, Y. J., You, Z. J., et al. (2003). Serum lysophosphatidic acid concentrations measured by dot immunogold filtration assay in patients with acute myocardial infarction. *Scand. J. Clin. Lab. Invest.* 63, 497–504. doi:10.1080/00365510310003265.

Chen, Z., Zhang, N., Chu, H. Y., Yu, Y., Zhang, Z.-K., Zhang, G., et al. (2020). Connective Tissue Growth Factor: From Molecular Understandings to Drug Discovery . *Front. Cell Dev. Biol.* 8. Available at: https://www.frontiersin.org/article/10.3389/fcell.2020.593269.

Contreras, O. (2020). Hic1 deletion unleashes quiescent connective tissue stem cells and impairs skeletal muscle regeneration. *J. Cell Commun. Signal.* 14, 131–133. doi:10.1007/s12079-019-00545-3.

Contreras, O., Córdova-Casanova, A., and Brandan, E. (2021a). PDGF-PDGFR network differentially regulates the fate, migration, proliferation, and cell cycle progression of myogenic cells. *Cell. Signal.* 84, 110036. doi:10.1016/j.cellsig.2021.110036.

Contreras, O., Cruz-Soca, M., Theret, M., Soliman, H., Tung, L. W., Groppa, E., et al. (2019). Cross-talk between TGF-β and PDGFRα signaling pathways regulates the fate of stromal fibro-adipogenic progenitors. *J. Cell Sci.* 132, jcs232157. doi:10.1242/jcs.232157.

Contreras, O., Rossi, F. M. V, and Theret, M. (2021b). Origins, potency, and heterogeneity of skeletal muscle fibro-adipogenic progenitors-time for new definitions. *Skelet Muscle* 11, 16. doi:10.1186/s13395-021-00265-6.

Contreras, O., Soliman, H., Theret, M., Rossi, F. M. V., and Brandan, E. (2020). TGF-β-driven downregulation of the transcription factor TCF7L2 affects Wnt/β-catenin signaling in PDGFRα+ fibroblasts. *J. Cell Sci.* 133. doi:10.1242/jcs.242297.

Córdova-Casanova, A., Cruz-Soca, M., Chun, J., Casar, J. C., and Brandan, E. (2022). Activation of the ATX/LPA/LPARs axis induces a fibrotic response in skeletal muscle. *Matrix Biol.* 109, 121–139. doi:https://doi.org/10.1016/j.matbio.2022.03.008.

D'Souza, K., Nzirorera, C., Cowie, A. M., Varghese, G. P., Trivedi, P., Eichmann, T. O., et al. (2018). Autotaxin-LPA signaling contributes to obesity-induced insulin resistance in muscle and impairs mitochondrial metabolism. *J. Lipid Res.* 59, 1805–1817. doi:https://doi.org/10.1194/jlr.M082008.

Davies, M. R., Lee, L., Feeley, B. T., Kim, H. T., and Liu, X. (2017). Lysophosphatidic acid-induced RhoA signaling and prolonged macrophage infiltration worsens fibrosis and fatty infiltration following rotator cuff tears. *J. Orthop. Res.* 35, 1539–1547. doi:https://doi.org/10.1002/jor.23384.

Decato, B. E., Leeming, D. J., Sand, J. M. B., Fischer, A., Du, S., Palmer, S. M., et al. (2022). LPA1 antagonist BMS-986020 changes collagen dynamics and exerts antifibrotic effects in vitro and in patients with idiopathic pulmonary fibrosis. *Respir. Res.* 23, 61. doi:10.1186/s12931-022-01980-4.

Dusaulcy, R., Rancoule, C., Grès, S., Wanecq, E., Colom, A., Guigné, C., et al. (2011). Adipose-specific disruption of autotaxin enhances nutritional fattening and reduces plasma lysophosphatidic acid. *J. Lipid Res.* 52, 1247–1255. doi:https://doi.org/10.1194/jlr.M014985.

Fang, X., Yu, S., Lapushin, R., Lu, Y., Furui, T., Penn, L. Z., et al. (2000). Lysophosphatidic acid prevents apoptosis in fibroblasts via Gi-protein-mediated activation of mitogen-activated protein kinase. *Biochem. J.* 352, 135–143. doi:10.1042/bj3520135.

Federico, L., Ren, H., Mueller, P. A., Wu, T., Liu, S., Popovic, J., et al. (2012). Autotaxin and Its Product Lysophosphatidic Acid Suppress Brown Adipose Differentiation and Promote Diet-Induced Obesity in Mice. *Mol. Endocrinol.* 26, 786–797. doi:10.1210/me.2011-1229.

Ferry, G., Tellier, E., Try, A., Grés, S., Naime, I., Simon, M. F., et al. (2003). Autotaxin Is Released from Adipocytes, Catalyzes Lysophosphatidic Acid Synthesis, and Activates Preadipocyte Proliferation: UP-REGULATED EXPRESSION WITH ADIPOCYTE DIFFERENTIATION AND OBESITY*. *J. Biol. Chem.* 278, 18162–18169. doi:https://doi.org/10.1074/jbc.M301158200.

Fry, C. S., Lee, J. D., Mula, J., Kirby, T. J., Jackson, J. R., Liu, F., et al. (2015). Inducible depletion of satellite cells in adult, sedentary mice impairs muscle regenerative capacity without affecting sarcopenia. *Nat. Med.* 21, 76–80. doi:10.1038/nm.3710.

Funcke, J.-B., and Scherer, P. E. (2019). Beyond adiponectin and leptin: adipose tissue-derived mediators of inter-organ communication. *J. Lipid Res.* 60, 1648–1697. doi:https://doi.org/10.1194/jlr.R094060.

Gan, L., Xue, J.-X., Li, X., Liu, D.-S., Ge, Y., Ni, P.-Y., et al. (2011). Blockade of lysophosphatidic acid receptors LPAR1/3 ameliorates lung fibrosis induced by irradiation. *Biochem. Biophys. Res. Commun.* 409, 7–13. doi:https://doi.org/10.1016/j.bbrc.2011.04.084.

Geraldo, L. H. M., Spohr, T. C. L. de S., Amaral, R. F. do, Fonseca, A. C. C. da, Garcia, C., Mendes, F. de A., et al. (2021). Role of lysophosphatidic acid and its receptors in health and disease: novel therapeutic strategies. *Signal Transduct. Target. Ther.* 6, 45. doi:10.1038/s41392-020-00367-5.

Giuliani, G., Rosina, M., and Reggio, A. (2021). Signaling pathways regulating the fate of fibro/adipogenic progenitors (FAPs) in skeletal muscle regeneration and disease. *FEBS J.* n/a. doi:https://doi.org/10.1111/febs.16080.

Gomez-Larrauri, A., Gangoiti, P., Presa, N., Dominguez-Herrera, A., Donati, C., Bruni, P., et al. (2021). Phosphatidic Acid Stimulates Myoblast Proliferation through Interaction with LPA1 and LPA2 Receptors. *Int. J. Mol. Sci.* 22. doi:10.3390/ijms22031452.

Harvey, T., Flamenco, S., and Fan, C. M. (2019). A Tppp3 + Pdgfra + tendon stem cell population contributes to regeneration and reveals a shared role for PDGF signalling in regeneration and fibrosis. *Nat. Cell Biol.* 21, 1490–1503. doi:10.1038/s41556-019-0417-z.

He, P., Haque, A., Lin, S., Cominelli, F., and Yun, C. C. (2018). Inhibition of autotaxin alleviates inflammation and increases the expression of sodium-dependent glucose cotransporter 1 and Na + /H + exchanger 3 in SAMP1/Fc mice. *Am. J. Physiol. Liver Physiol.* 315, G762–G771. doi:10.1152/ajpgi.00215.2018.

HEUSINGER-RIBEIRO, J., EBERLEIN, M., WAHAB, N. A., and GOPPELT-STRUEBE, M. (2001). Expression of Connective Tissue Growth Factor in Human Renal Fibroblasts: Regulatory Roles of RhoA and cAMP. *J. Am. Soc. Nephrol.* 12, 1853–1861. doi:10.1681/ASN.V1291853.

Jean-Baptiste, G., Yang, Z., Khoury, C., and Greenwood, M. T. (2005). Lysophosphatidic acid mediates pleiotropic responses in skeletal muscle cells. *Biochem. Biophys. Res. Commun.* 335, 1155–1162. doi:https://doi.org/10.1016/j.bbrc.2005.08.011.

Kihara, Y., Maceyka, M., Spiegel, S., and Chun, J. (2014). Lysophospholipid receptor nomenclature review: IUPHAR Review 8. *Br. J. Pharmacol.* 171, 3575–3594. doi:https://doi.org/10.1111/bph.12678.

Lepper, C., Partridge, T. A., and Fan, C.-M. (2011). An absolute requirement for Pax7-positive satellite cells in acute injury-induced skeletal muscle regeneration. *Development*. doi:10.1242/dev.067595.

Lidgerwood, G. E., Pitson, S. M., Bonder, C., and Pébay, A. (2018). Roles of lysophosphatidic acid and sphingosine-1-phosphate in stem cell biology. *Prog. Lipid Res.* 72, 42–54. doi:https://doi.org/10.1016/j.plipres.2018.09.001.

Magkrioti, C., Oikonomou, N., Kaffe, E., Mouratis, M.-A., Xylourgidis, N., Barbayianni, I., et al. (2018). The Autotaxin—Lysophosphatidic Acid Axis Promotes Lung Carcinogenesis. *Cancer Res.* 78, 3634–3644. doi:10.1158/0008-5472.CAN-17-3797.

Molina, T., Fabre, P., and Dumont, N. A. (2022). Fibro-adipogenic progenitors in skeletal muscle homeostasis, regeneration and diseases. *Open Biol.* 11, 210110. doi:10.1098/rsob.210110.

Moolenaar, W. H. (1995). Lysophosphatidic Acid, a Multifunctional Phospholipid Messenger ∗ *J. Biol. Chem.* 270, 12949–12952. doi:10.1074/jbc.270.22.12949.

Morales, M. G., Gutierrez, J., Cabello-Verrugio, C., Cabrera, D., Lipson, K. E., Goldschmeding, R., et al. (2013). Reducing CTGF/CCN2 slows down mdx muscle dystrophy and improves cell therapy. *Hum. Mol. Genet.* doi:10.1093/hmg/ddt352.

Murphy, M. M., Lawson, J. A., Mathew, S. J., Hutcheson, D. A., and Kardon, G. (2011). Satellite cells, connective tissue fibroblasts and their interactions are crucial for muscle regeneration. *J. Cell Sci.* 124, e1–e1. doi:10.1242/jcs098228.

Ninou, I., Magkrioti, C., and Aidinis, V. (2018). Autotaxin in Pathophysiology and Pulmonary Fibrosis . *Front. Med.* 5. Available at: https://www.frontiersin.org/article/10.3389/fmed.2018.00180.

Nishimura, S., Nagasaki, M., Okudaira, S., Aoki, J., Ohmori, T., Ohkawa, R., et al. (2014). ENPP2 Contributes to Adipose Tissue Expansion and Insulin Resistance in Diet-Induced Obesity. *Diabetes* 63, 4154–4164. doi:10.2337/db13-1694.

Ohashi, T., and Yamamoto, T. (2015). Antifibrotic effect of lysophosphatidic acid receptors LPA1 and LPA3 antagonist on experimental murine scleroderma induced by bleomycin. *Exp. Dermatol.* 24, 698–702. doi:https://doi.org/10.1111/exd.12752.

Okudaira, S., Yukiura, H., and Aoki, J. (2010). Biological roles of lysophosphatidic acid signaling through its production by autotaxin. *Biochimie* 92, 698–706. doi:https://doi.org/10.1016/j.biochi.2010.04.015.

Oprescu, S. N., Yue, F., and Kuang, S. (2020). Single-Cell Isolation from Regenerating Murine Muscles for RNA-Sequencing Analysis. *STAR Protoc.* 1, 100051. doi:10.1016/j.xpro.2020.100051.

Petrosino, J. M., Leask, A., and Accornero, F. (2018). Genetic manipulation of CCN2/CTGF unveils cell-specific ECM-remodeling effects in injured skeletal muscle. *FASEB J.* 33, 2047–2057. doi:10.1096/fj.201800622RR.

Petrosino, J. M., Leask, A., and Accornero, F. (2019). Genetic manipulation of CCN2/CTGF unveils cell-specific ECM-remodeling effects in injured skeletal muscle. *FASEB J.* 33, 2047–2057. doi:10.1096/fj.201800622RR.

Ray, R., Sinha, S., Aidinis, V., and Rai, V. (2021). Atx regulates skeletal muscle regeneration via LPAR1 and promotes hypertrophy. *Cell Rep.* 34, 108809. doi:https://doi.org/10.1016/j.celrep.2021.108809.

Rebolledo, D. L., Gonzalez, D., Faundez-Contreras, J., Contreras, O., Vio, C. P., Murphy-Ullrich, J. E., et al. (2019). Denervation-induced skeletal muscle fibrosis is mediated by CTGF/CCN2 independently of TGF-beta. *Matrix Biol.* 82, 20–37. doi:10.1016/j.matbio.2019.01.002.

Riquelme-Guzmán, C., Contreras, O., and Brandan, E. (2018). Expression of CTGF/CCN2 in response to LPA is stimulated by fibrotic extracellular matrix via the integrin/FAK axis. *Am. J. Physiol. - Cell Physiol.* doi:10.1152/ajpcell.00013.2017.

Sah, J. P., Hao, N. T. T., Han, X., Tran, T. T. T., McCarthy, S., Oh, Y., et al. (2020). Ectonucleotide pyrophosphatase 2 (ENPP2) plays a crucial role in myogenic differentiation through the regulation by WNT/β-Catenin signaling. *Int. J. Biochem. Cell Biol.* 118, 105661. doi:https://doi.org/10.1016/j.biocel.2019.105661.

Sakai, N., Chun, J., Duffield, J. S., Wada, T., Luster, A. D., and Tager, A. M. (2013). LPA1-induced cytoskeleton reorganization drives fibrosis through CTGF-dependent fibroblast proliferation. *FASEB J.* 27, 1830–1846. doi:https://doi.org/10.1096/fj.12-219378.

Sambasivan, R., Yao, R., Kissenpfennig, A., van Wittenberghe, L., Paldi, A., Gayraud-Morel, B., et al. (2011). Pax7-expressing satellite cells are indispensable for adult skeletal muscle regeneration. *Development* 138, 3647–3656. doi:10.1242/dev.067587.

Scott, R. W., Arostegui, M., Schweitzer, R., Rossi, F. M. V., and Underhill, T. M. (2019). Hic1 Defines Quiescent Mesenchymal Progenitor Subpopulations with Distinct Functions and Fates in Skeletal Muscle Regeneration. *Cell Stem Cell*. doi:10.1016/j.stem.2019.11.004.

Soliman, H., Paylor, B., Scott, R. W., Lemos, D. R., Chang, C., Arostegui, M., et al. (2020). Pathogenic Potential of Hic1-Expressing Cardiac Stromal Progenitors. *Cell Stem Cell* 26, 205-220.e8. doi:10.1016/j.stem.2019.12.008.

Stortelers, C., Kerkhoven, R., and Moolenaar, W. H. (2008). Multiple actions of lysophosphatidic acid on fibroblasts revealed by transcriptional profiling. *BMC Genomics* 9, 387. doi:10.1186/1471-2164-9-387.

Tager, A. M., LaCamera, P., Shea, B. S., Campanella, G. S., Selman, M., Zhao, Z., et al. (2008). The lysophosphatidic acid receptor LPA1 links pulmonary fibrosis to lung injury by mediating fibroblast recruitment and vascular leak. *Nat. Med.* 14, 45–54. doi:10.1038/nm1685.

Tanaka, M., Okudaira, S., Kishi, Y., Ohkawa, R., Iseki, S., Ota, M., et al. (2006). Autotaxin Stabilizes Blood Vessels and Is Required for Embryonic Vasculature by Producing Lysophosphatidic Acid*. *J. Biol. Chem.* 281, 25822–25830. doi:https://doi.org/10.1074/jbc.M605142200.

Tang, X., Benesch, M. G. K., and Brindley, D. N. (2015). Lipid phosphate phosphatases and their roles in mammalian physiology and pathology. *J. Lipid Res.* 56, 2048–2060. doi:10.1194/jlr.R058362.

Tang, X., and Brindley, D. N. (2020). Lipid Phosphate Phosphatases and Cancer. *Biomol.* 10. doi:10.3390/biom10091263.

Theret, M., Rossi, F. M. V., and Contreras, O. (2021). Evolving Roles of Muscle-Resident Fibro-Adipogenic Progenitors in Health, Regeneration, Neuromuscular Disorders, and Aging. *Front. Physiol.* 12, 1–23. doi:10.3389/fphys.2021.673404.

Tokumura, A., Majima, E., Kariya, Y., Tominaga, K., Kogure, K., Yasuda, K., et al. (2002). Identification of Human Plasma Lysophospholipase D, a Lysophosphatidic Acid-producing Enzyme, as Autotaxin, a Multifunctional Phosphodiesterase*. *J. Biol. Chem.* 277, 39436–39442. doi:https://doi.org/10.1074/jbc.M205623200.

Umezu-Goto, M., Kishi, Y., Taira, A., Hama, K., Dohmae, N., Takio, K., et al. (2002). Autotaxin has lysophospholipase D activity leading to tumor cell growth and motility by lysophosphatidic acid production . *J. Cell Biol.* 158, 227–233. doi:10.1083/jcb.200204026.

van Corven, E. J., Groenink, A., Jalink, K., Eichholtz, T., and Moolenaar, W. H. (1989). Lysophosphatidate-induced cell proliferation: Identification and dissection of signaling pathways mediated by G proteins. *Cell* 59, 45–54. doi:https://doi.org/10.1016/0092-8674(89)90868-4.

van Corven, E. J., van Rijswijk, A., Jalink, K., van der Bend, R. L., van Blitterswijk, W. J., and Moolenaar, W. H. (1992). Mitogenic action of lysophosphatidic acid and phosphatidic acid on fibroblasts. Dependence on acyl-chain length and inhibition by suramin. *Biochem. J.* 281, 163–169. doi:10.1042/bj2810163.

Vial, C., Zúñiga, L. M., Cabello-Verrugio, C., Cañón, P., Fadic, R., and Brandan, E. (2008). Skeletal muscle cells express the profibrotic cytokine connective tissue growth factor (CTGF/CCN2), which induces their dedifferentiation. *J. Cell. Physiol.* 215, 410–421. doi:10.1002/jcp.21324.

Xu, F., Deng, C., Ren, Z., Sun, L., Meng, Y., Liu, W., et al. (2021). Lysophosphatidic acid shifts metabolic and transcriptional landscapes to induce a distinct cellular state in human pluripotent stem cells. *Cell Rep.* 37. doi:10.1016/j.celrep.2021.110063.

Xu, Y.-J., Tappia, P. S., Goyal, R. K., and Dhalla, N. S. (2008). Mechanisms of the lysophosphatidic acid-induced increase in [Ca2+]i in skeletal muscle cells. *J. Cell. Mol. Med.* 12, 942–954. doi:https://doi.org/10.1111/j.1582-4934.2008.00139.x.

Yoshida, S., Fujisawa-Sehara, A., Taki, T., Arai, K., and Nabeshima, Y. (1996). Lysophosphatidic acid and bFGF control different modes in proliferating myoblasts. *J. Cell Biol.* 132, 181–193. doi:10.1083/jcb.132.1.181.

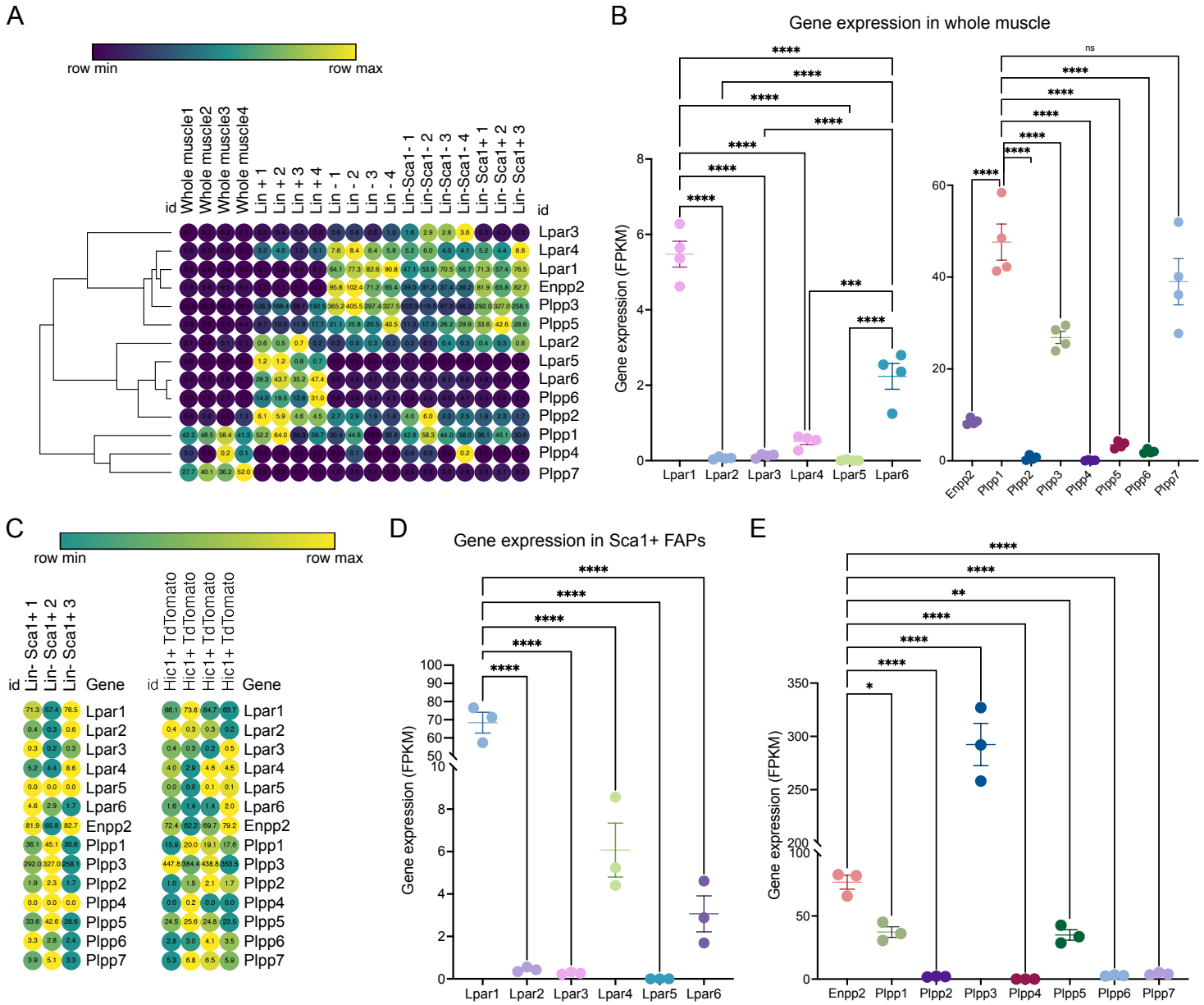

Figure 1. Bulk RNAseq transcriptomics analysis revealed differential gene expression of the LPA-LPAR-Autotaxin-Plpp network. (A) Heat map showing gene expression levels of Lpar, Enpp2, and Plpp genes in whole skeletal muscle tissue, Lineage$^+$, Lineage$^-$, and Lineage$^-$Sca1$^+$ FAPs from a bulk RNAseq library [Scott et al., 2019]. Gene expression is shown as fragments per kilobase of exon per million mapped fragments (FPKM). (B) Quantification of Lpar, Enpp2, and Plpp genes transcript abundance (FPKM) in muscle tissue. (C) Heat map showing gene expression levels of Lpar, Enpp2, and Plpp genes in Lineage$^-$Sca1$^+$ FAPs and Hic1+ tdTomato expressing cells [Scott et al., 2019]. (D) Quantification of Lpar$_{(1-6)}$genes transcript abundance (FPKM) in Sca1$^+$ FAPs. (E) Quantification of Enpp2 and Plpp genes transcript abundance (FPKM) in Sca1$^+$ FAPs.

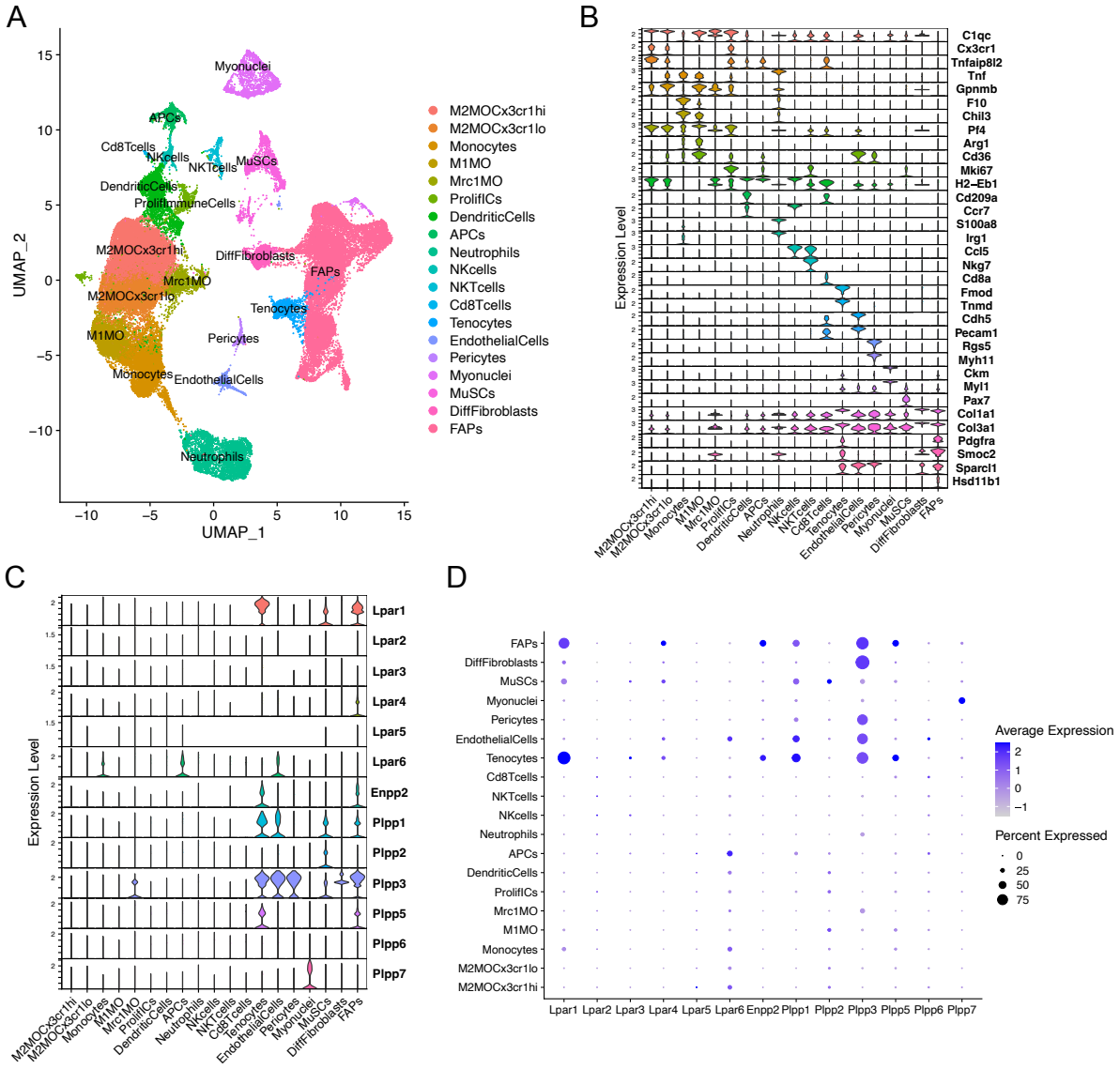

Figure 2. Analysis of LPAR-Autotaxin/Enpp2-Plpp gene expression at single-cell resolution. (A) Uniform manifold approximation and projection (UMAP) plot of scRNA-seq public data [Oprescu et al., 2020] showing 19 distinct cell lineages in single cells across skeletal muscle homeostasis and regeneration. Detected major cell lineages were colored by the predominant cell type(s) that composes each cluster. (B) Violin plots showing the expression level of several marker genes across the different populations depicted in (A). (C) Violin plots showing the gene expression level of LPAR, Enpp2, and Plpp family members across the different populations or cell clusters. (D) Dot plot showing gene expression levels of LPAR, Enpp2, and Plpp family members. Dot plots help to visualize two values across two dimensions: color and size. The color gradient of the dot approximates average gene expression (light grey: low expression; Navy blue: high expression). Dot size represents the

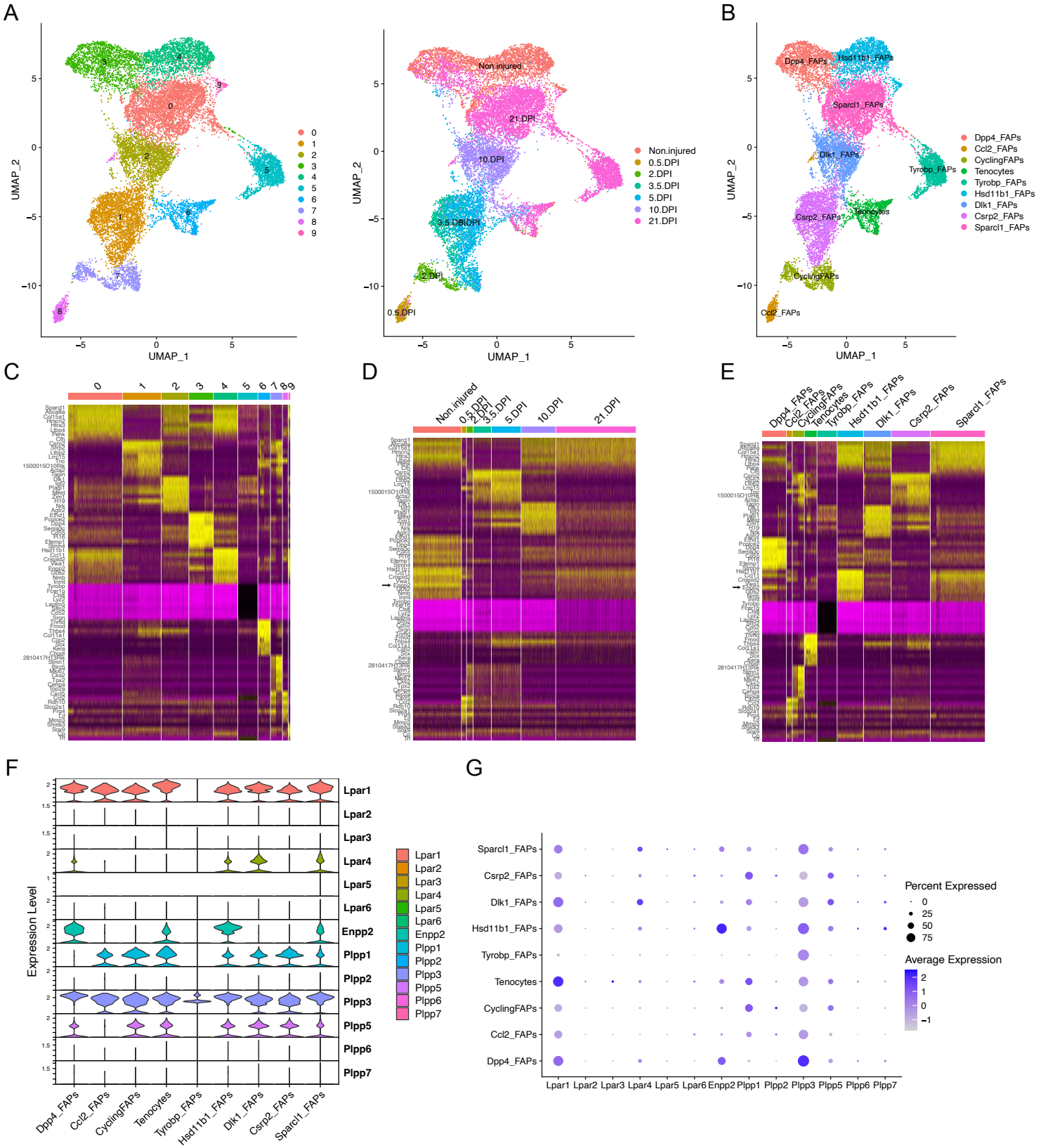

Figure 3. Resting fibro-adipogenic progenitors predominantly express LPA receptors and LPA-producing enzyme Enpp2/Autotaxin. (A) UMAP plot showing 10 distinct clusters across skeletal muscle homeostasis and regeneration when subclustering FAPs, DiffFibroblasts, and tenocytes subclusters. Detected major cell lineages and states were colored by the predominant cell type(s) that composes each cluster (0-9). (B) UMAP plot showing 9 distinct clusters (8 clusters for FAP lineage and 1 for tenocytes), which are named based on the most highly expressed gene shown in the heat maps shown below (C, E). (C) Heat map plot showing *top 8* expressed genes in each individual initial cluster shown in (A). (D) Heat map plot showing *top 8* expressed genes in the grouped 9 distinct clusters at different conditions (undamaged and days post-injury [DPI]). (E) Heat map plot showing the named clusters as described in the text, having its name because of one of the *top 8* expressed genes in each subset. (E) UMAP plot showing individual cells grouped based on the different conditions (uninjured and injured muscle) at different time points. DPI: days post-injury. (F) Violin plots showing the gene expression level of LPAR, Enpp2, and Plpp family members across the different FAPs and tenocytes subclusters. (G) Dot plot showing gene expression levels of LPAR, Enpp2, and Plpp family members. Note that Dpp4 and Hsd11b1 FAPs highly express *Enpp2*/ATX gene.

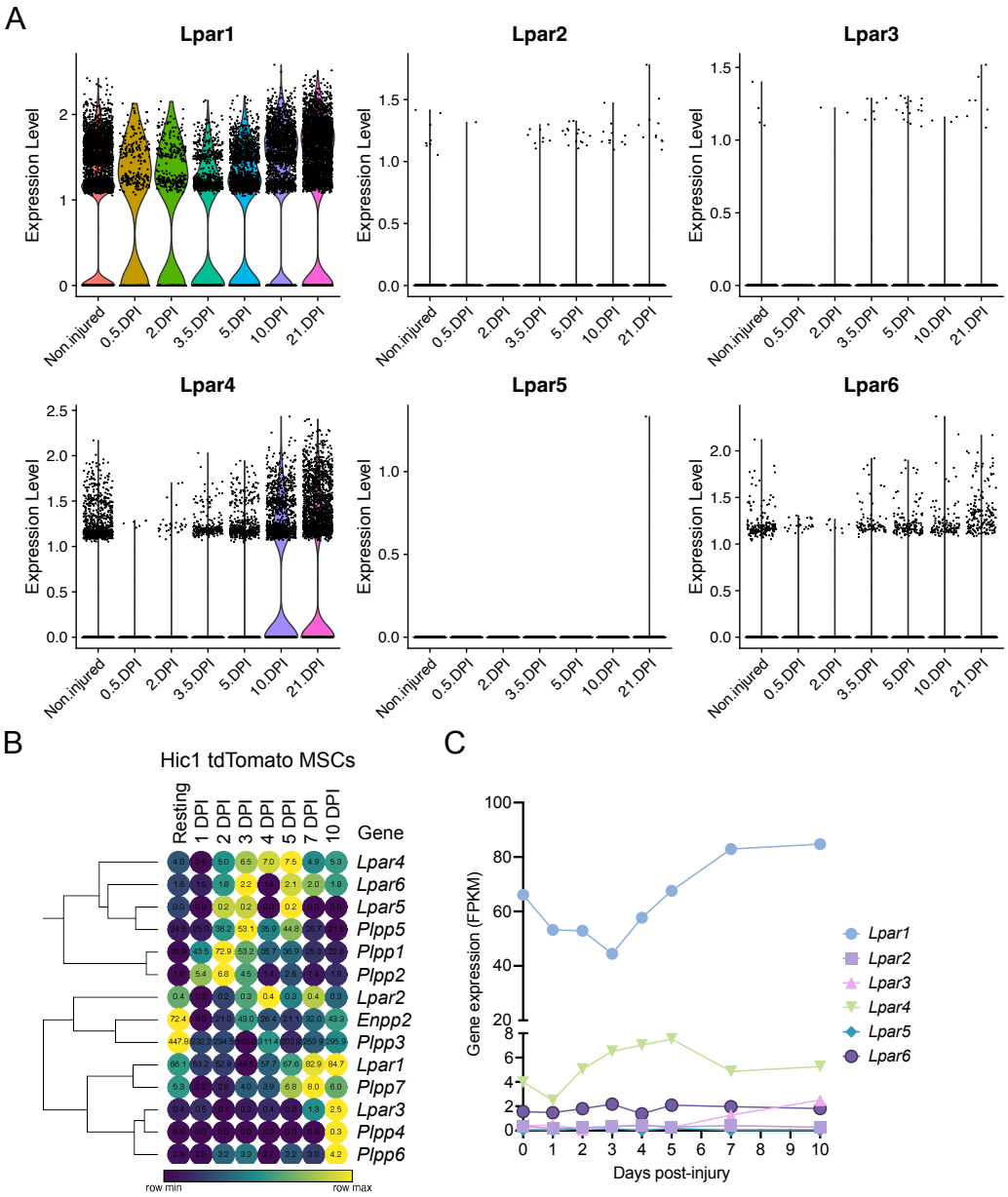

Figure 4. Muscle injury triggers a fast and strong downregulation LPA receptors in fibro-adipogenic progenitors. (A) Violin plots showing the gene expression level of LPAR family members and dynamics in response to injury. DPI: Days post-injury. (B) Heat map showing gene expression levels of Lpar, Enpp2, and Plpp genes in Hic1+ tdTomato expressing cells upon acute muscle damage [Scott et al., 2019]. (C) Quantification of $Lpar_{(1-6)}$ genes transcript abundance (FPKM) in Hic1+ tdTomato expressing cells and dynamics in response to injury. DPI: Days post-injury.

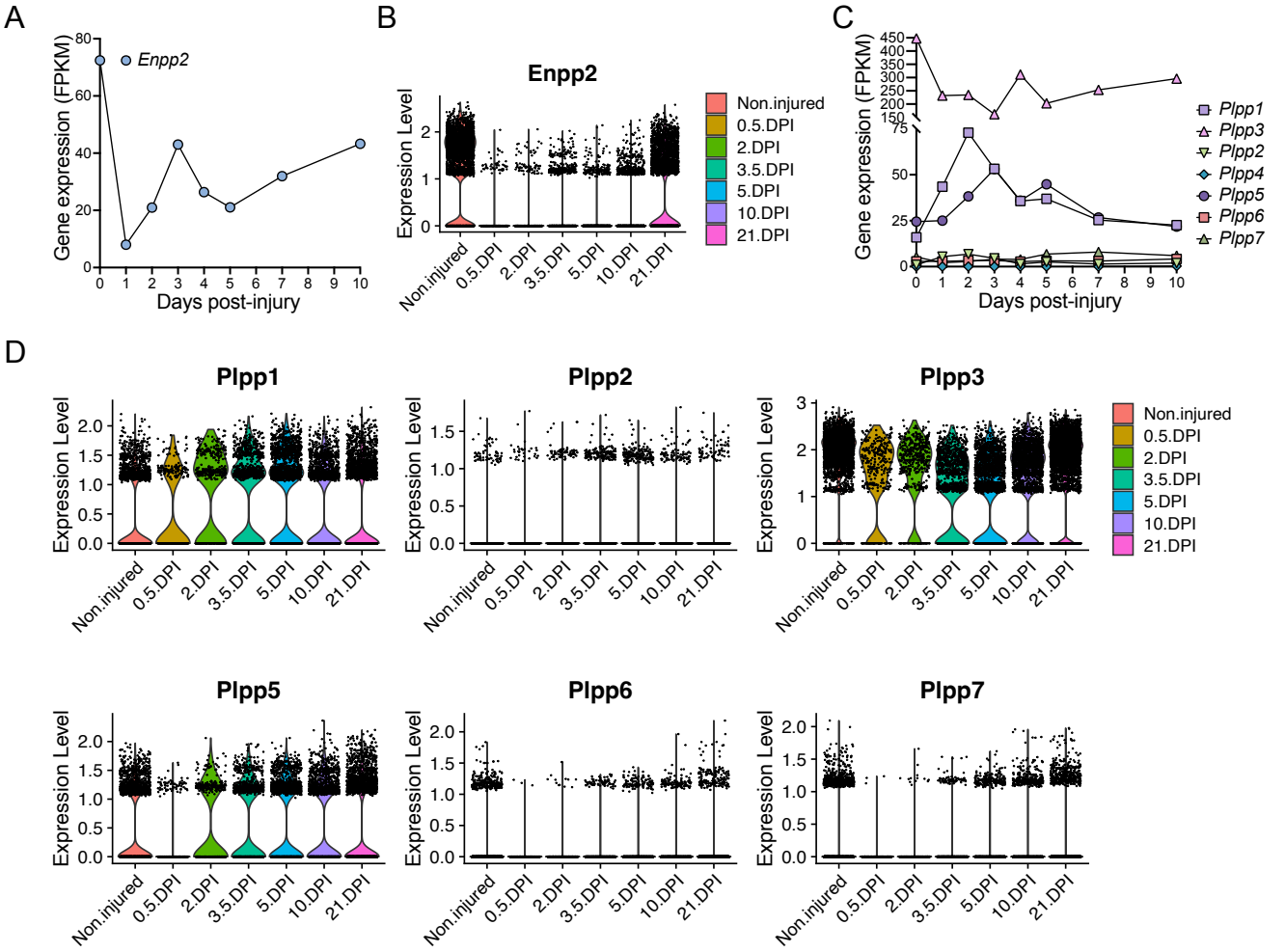

Figure 5. Quick and pronounced gene repression of LPA-producing and -catabolizing enzymes in fibro-adipogenic progenitors following muscle damage. (A) Quantification of Enpp2 transcript abundance (FPKM) in Hic1+ tdTomato expressing cells in response to injury. (B) Violin plots showing the gene expression level of *Enpp2* in FAPs in response to injury . DPI: Days post-injury. (C) Quantification of different Plpps transcript abundance (FPKM) in Hic1+ tdTomato expressing cells in response to injury. (D) Violin plots showing the expression level of the seven *Plpp* genes in FAPs in response to injury. DPI: Days post-injury.

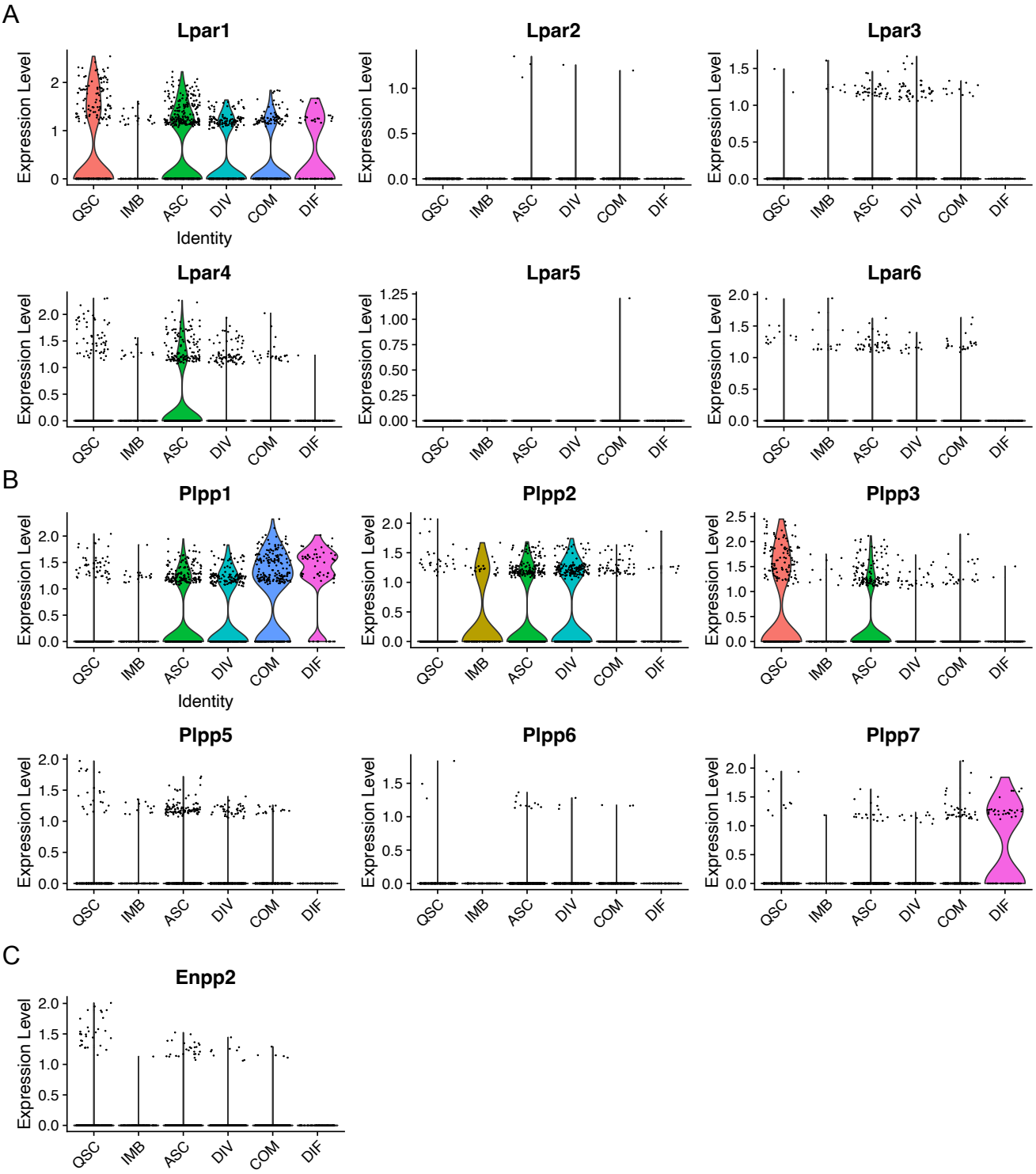

Figure 6. Upregulation of Lpar1 and Lpar4 associates with an activated muscle stem cell subpopulation.
(A-C) Violin plots showing the gene expression level of LPAR (A), Plpp (B), and Enpp2 (C) family members across the different MuSCs subpopulations Abbreviations: DIF, differentiated MuSCs; COM, committed MuSCs; DIV, dividing MuSCs; ASC, activated MuSCs; IMB, immunomyoblasts; QSC, quiescent MuSCs.